Oxidation of 4-Methylanisole by Aqueous Cerium(IV) in a Two−Phase Immiscible Liquid/Liquid System: Interfacial versus Homogeneous Control

Christopher J. Slevin, Jie Zhang, and Patrick R. Unwin*

Department of Chemistry, University of Warwick, Coventry, United Kingdom CV4 7AL

Received: October 16, 2001

The kinetics of the oxidation of 4-methylanisole (MA) by Ce(IV) have been measured in both two-phase (MA/aqueous sulfuric acid) and single-phase (aqueous sulfuric acid) arrangements by using microelectrochemical measurements at expanding droplets (MEMED) and UV−visible spectrophotometry, respectively. In the two-phase arrangement, the electron transfer (ET) reaction appeared to occur interfacially, rather than by dissolution of MA followed by reaction in solution as previously considered. The effective first-order rate constant for the consumption of Ce(IV) at the interface is 2.0×10^{-4} cm s^{-1}. The homogeneous reaction is first-order in both Ce(IV) and MA, with a rate constant for the loss of Ce(IV) of 1.0 mol^{-1} dm^3 s^{-1}. The lifetime of the 4-methylanisole radical cation in aqueous sulfuric acid, formed in the first step of the oxidation process, has been measured independently as ∼10 ms using steady-state ultramicroelectrode voltammetry. The factors leading to the different energetics of the one phase and interfacial reaction are discussed, and the implications of the observed kinetics on scale-up are highlighted.

Introduction

A wide range of reactions of importance in synthesis and process chemistry, such as phase transfer catalysis[1] and extraction processes,[2,3] involve conditions where the reagents are initially in two different immiscible liquid phases. The oxidation of 4-methylanisole (MA), by aqueous acidic solutions of Ce(IV), is an example of a reaction from synthetic organic chemistry which is conducted in such a two-phase arrangement.[4−6] This is one of a class of reactions in which relatively powerful oxidizing agents such as 12-tungstocobalt(III)ate,[7,8] nitrate radical, tris(phenanthroline)iron(III), tris(bipyridine)ruthenium(III), and Ce(IV)[4−6,12−17] are used (in single- or dual-phase systems) to facilitate the oxidation of alkyl aromatics. Two-phase liquid/liquid systems offer some advantages over single-phase methods, in that the aqueous phase containing the spent redox mediator may be easily separated and passed over an electrode to regenerate the active redox species, and product separation is also simplified.[4−6]

The oxidation of MA by Ce(IV) in a two-phase arrangement, with recycling of the oxidant, has been the subject of detailed studies.[4−6] The redox reaction was proposed to occur in the aqueous phase after dissolution of MA from the pure organic liquid (Figure 1). The products were considered to be extracted into the organic phase, and further oxidation was possible by dissolution and reaction. In these investigations the kinetic factors determining the product distribution were a major concern,[4−6] and all of the chemical reactions were assumed to occur homogeneously in the aqueous phase. The possibility of any interfacial redox reaction was not considered, although there is now increasing evidence from other studies that many electron transfer (ET) reactions occur across the interface between immiscible liquid phases.[18,19]

This paper describes the application of microelectrochemical measurements at expanding droplets (MEMED)[20,21] to study the oxidation of MA by Ce(IV) in a two-phase system. MEMED is a recent development for resolving the kinetics of spontaneous reactions at liquid/liquid interfaces under conditions of well-defined mass transport and controlled interfacial contact. In contrast to earlier techniques,[1,3,21,22] MEMED is unique in that the reactant and/or product concentration profiles adjacent to a liquid/liquid interface are measured directly, enabling the determination of whether a reaction is truly homogeneous, interfacial, or in a mixed regime.

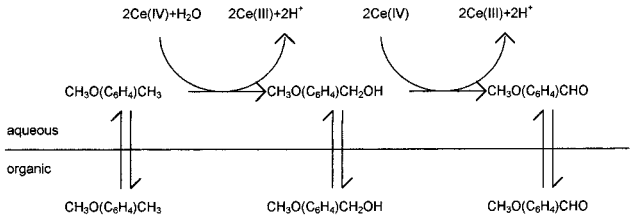

Figure 1. Schematic representation of the two-phase reaction between pure 4-methylanisole (organic phase) and Ce(IV) in aqueous sulfuric acid.

In the present study, MEMED has been used to measure the dissolution of MA in aqueous sulfuric acid electrolyte. The two-phase reaction between MA and Ce(IV) has been investigated by directly probing the concentration profiles for these two species, after introducing Ce(IV) into the bulk of an aqueous (receptor) phase. The kinetics for the homogeneous reaction between Ce(IV) and MA in aqueous solution have been measured separately using UV/visible spectrophotometry. Additionally, ultramicroelectrode voltammetry has been employed to determine the lifetime of the methylanisole radical cation in aqueous sulfuric acid. With this combined approach, in which the key steps in the oxidation process are characterized by complementary techniques, the various contributions of interfacial and homogeneous reactions can be fully assessed and rationalized for the first time.

It is important to emphasize the difference between the studies herein and previous investigations of ET across liquid/liquid

10.1021/jp013818v CCC: $22.00 © 2002 American Chemical Society
Published on Web 02/26/2002

interfaces.[18,19] In the latter area, a redox solute species is confined in each immiscible liquid phase and the ET reaction considered to occur across a sharp solvent plane[23] or mixed solvent region.[24] In the studies herein, we are interested in a situation where one of the redox species is actually a pure liquid phase (MA).

Experimental Section

Chemicals. All aqueous solutions were prepared from Milli-Q reagent water (Millipore Corp., resistivity ≥ 18 MΩ cm) and contained 4-methylanisole (99%, Sigma-Aldrich, Gillingham, U.K.), cerium(IV) sulfate (99%, Sigma-Aldrich), $NaClO_4 \cdot xH_2O$ (99.99%, Sigma−Aldrich) and sulfuric acid (A.R., specific gravity 1.84, Sigma-Aldrich) at the concentrations outlined herein.

Apparatus. The experimental arrangements and equipment for MEMED and voltammetric measurements have been described previously.[20,21] In the present application, amperometry was used to measure concentration profiles, as described elsewhere.[20b] MA formed the feeder phase, which was flowed through a fine tapered glass capillary (100-μm internal diameter) into an aqueous receptor phase. Flow rates in the range 25−85 μL min^{-1} were deployed by using a syringe pump (model KD100, C-P Instruments, Bishop's Stortford, U.K.) fitted with a 500-μL syringe (Hamilton Co., Gas Tight, Reno, NV). Pt UMEs with diameters of 1, 2, 10, 25, and 50 μm were fabricated and prepared according to previously described procedures and had a ratio of the overall tip diameter to that of the electroactive area, RG, of 10. All electrochemical measurements were made in a two-electrode arrangement with an UME as the working electrode and either a silver quasi-reference electrode (Ag QRE) or saturated calomel reference electrode (SCE).

To measure MA concentration profiles in MEMED, only the characteristic approach region of the transient was recorded, as it was found that the oxidation of MA at the electrode for long periods resulted in a diminution in the current flow, attributed to the deposition of products at the electrode surface. For this reason, the electrode was also polished between MEMED measurements, when required, as described elsewhere.[25]

UV/visible absorption spectra of aqueous sulfuric acid solutions of Ce(IV), Ce(III), and MA were measured by scanning between 400 and 900 nm using a spectrometer (8700 series, Unicam). Homogeneous kinetic measurements were made in a 4-mL volume quartz cuvette with a 1-cm path length in which the two reacting solutions were mixed. Absorbances for Ce(IV) were recorded at a fixed wavelength of 320 nm, which corresponded only to Ce(IV), as a function of time using an ATI Unicam, model 8625 spectrometer interfaced to a PC. All measurements were made at 23 ± 1 °C.

Results and Discussion

Voltammetry of MA and Ce(IV). As described below, the two-phase reaction was followed in the MEMED configuration by amperometric measurement of both MA and Ce(IV) at a 1-μm diameter Pt UME in an aqueous phase. The Ce(IV) concentration could be measured successfully by amperometry by biasing the UME at the potential for the diffusion-controlled reduction of Ce(IV), ca. 0.0 V vs AgQRE. The oxidation of Ce(III) occurs beyond the solvent window and could not be observed.

The diffusion coefficient, D, of Ce(IV) under these solution conditions was determined from the steady-state diffusion-limited current, i_{bulk}, for the reduction of Ce(IV) measured in separate experiments at both 25- and 1-μm diameter Pt UMEs positioned in the bulk of an aqueous solution containing 3.0 × 10^{-3} M Ce(IV) sulfate and 1.0 M sulfuric acid,

$$i_{bulk} = 4nFDac^* \quad (1)$$

where $n = 1$ is the number of electrons transferred, F is Faraday's constant, a is the radius of the UME, and c^* is the concentration. The diffusion coefficient, $D_{Ce(IV)} = 4.6\ (\pm 0.1) \times 10^{-6}$ cm^2 s^{-1} was found to be in reasonable agreement with the value measured previously by using a rotating disk electrode.[27]

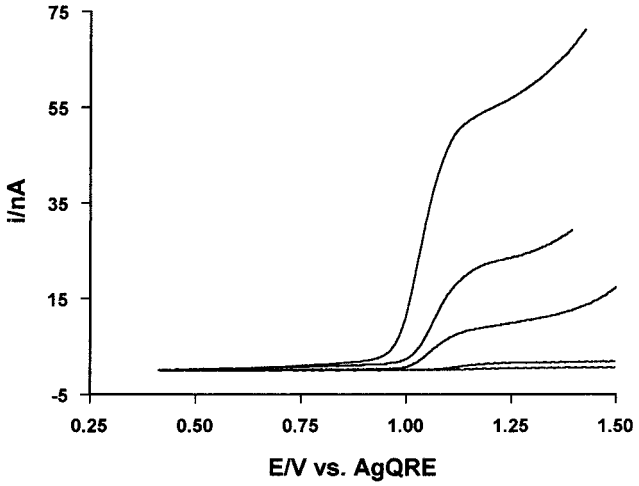

Figure 2. Steady-state voltammograms for the oxidation of MA at a range of Pt UMEs of diameter, bottom to top, 1, 2, 10, 25, and 50 μm. The aqueous solution was 1.0 M H_2SO_4 saturated with MA.

TABLE 1: Number of Electrons Transferred in the Oxidation of MA, Calculated from the Limiting Current, for a Range of UME Sizes

electrode radius/μm	n_{eff}
0.5	1.13
1.0	1.25
5.0	1.79
12.5	1.90
25.0	2.00

The voltammetry of MA is more complex, as revealed by the series of voltammograms in Figure 2, recorded at a range of UME sizes, $a = 0.5$, 1, 5, 12.5, and 25 μm in a 1.0 M sulfuric acid solution saturated with respect to MA. The ratio i_{lim}/a, which is invariant for simple diffusion-limited electron transfer (eq 1) shifts from larger to smaller values as the electrode size is decreased. The decrease in electrode size corresponds to an increase in the mean steady-state mass transfer coefficient:

$$k_t = \frac{4D}{\pi a} \quad (2)$$

Earlier rotating disk electrode (RDE) studies of MA oxidation at Pt under similar conditions found a two-electron process, invariant with rotation speed (up to 50 Hz).[4] The mass transfer coefficient for an RDE[28] at a rotation frequency of 50 Hz is about twice the mean mass transfer coefficient at a 50-μm diameter UME (eq 2), so that a 50-μm diameter UME may also be expected to show a two-electron process for MA oxidation. The effective number of electrons transferred, n_{eff}, for the other electrode sizes may then be calculated from the limiting currents, resulting in the values shown in Table 1. The apparent trend of decreasing n_{eff}, between two and one electrons, with increasing k_t is indicative of an electrode process in which two single electron transfer steps are coupled to an interposed homogeneous

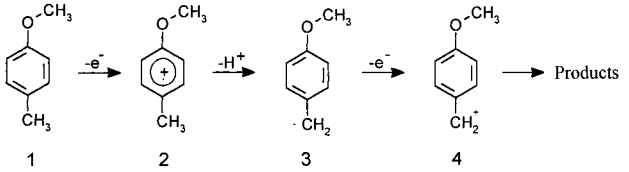

Figure 3. Proposed ECE mechanism for the electrochemical oxidation of methylanisole.

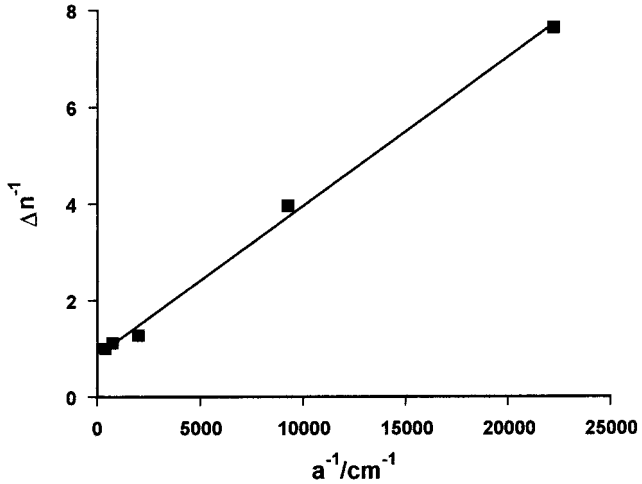

Figure 4. Analysis of the limiting current data in Figure 2 in terms of eqs 3 or 4 to determine the rate constant for the homogeneous chemical step (deprotonation of the methylanisole radical cation), assuming an ECE or DISP1 process describes the oxidation of MA at the electrode.

solution reaction.[29] This observation is consistent with previous studies of the oxidation of MA in a range of solvents, including acetic acid/water,[8,12] methanol,[16] sulfuric acid/acetone,[30] and acetonitrile,[31] which was considered to occur via a general "ECE" scheme (Figure 3), for situations where the initial ET step occurred either with an oxidant in solution[8,12,13,16] or heterogeneously at an electrode surface.[30−32]

For the anodic oxidation process considered here, the heterogeneous transfer of one electron from MA at the electrode results in the formation of the cation radical which undergoes deprotonation (C step), before a second electron is lost at the electrode (E step) or in solution (via disproportionation). The experimental results are consistent with this; i.e., as the transport rate is increased, with the use of smaller electrodes, the C step becomes increasingly slow compared to mass transport and the second electron−transfer step occurs to a lesser extent.

If the results are interpreted in terms of an ECE mechanism, the rate constant, k_{ECE}, for the chemical step can be determined from[33]

$$\frac{1}{\Delta n} = \frac{4}{\pi a}\left(\frac{D}{n_2^2 k_{ECE}}\right)^{1/2} + \frac{1}{n_2} \qquad (3)$$

In eq 3, $\Delta n = n_{eff} - n_1$, where n_{eff} is the effective total number of electrons transferred, $n_1 = 1$ is the number of electrons transferred in the first step, $n_2 = 1$ is the number of electrons transferred in the second step, and D is the diffusion coefficient of MA. The plot of Δn^{-1} vs a^{-1} in Figure 4, indicates that this analysis provides a good description of the limiting current data for the oxidation of MA. The resulting rate constant for the deprotonation reaction was $k_{ECE} = 77 \pm 5\ s^{-1}$ from the slope of the line.

Alternatively, a DISP1 mechanism may also account for the observed behavior,[29] in which species 2 and 3 in the schematic

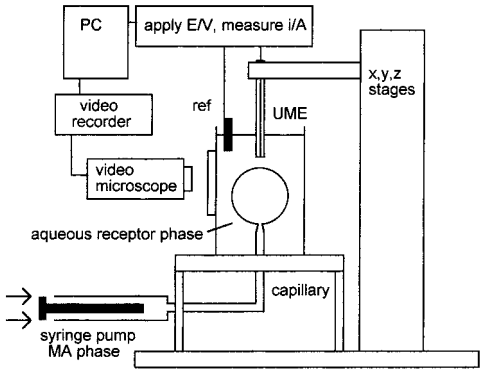

Figure 5. Experimental arrangement for MEMED measurements.

in Figure 3 react to produce species 1 and 4, with step 2 still rate-limiting. The rate constant may then be calculated from[33]

$$\frac{1}{\Delta n} = \frac{4}{\pi a}\left(\frac{2D}{n_1^2 k_{DISP1}}\right)^{1/2} + \frac{1}{n_1} \qquad (4)$$

resulting in $k_{DISP1} = 154 \pm 10\ s^{-1}$. Whichever mechanism holds, ECE or DISP1, the MA radical cation is relatively short-lived with a lifetime ~10 ms.

Despite the complicated voltammetry for the oxidation of MA, its concentration measurement in the MEMED arrangement is still possible by diffusion-limited amperometry at a 1-μm diameter Pt UME, which has a constant mass transport rate.

Dissolution of MA from an Expanding Droplet in Aqueous Solution. Since the oxidation of MA by aqueous sulfuric acid solutions of Ce(IV) has been considered to occur via the dissolution of MA into aqueous solution, followed by a homogeneous oxidation reaction,[4−6] the dissolution of MA from drops of the neat reactant was first measured by the MEMED method. Since MA has a slightly lower density than water, $\rho_{MA} = 0.969$ g cm^{-3}, the capillary carrying the MA feeder phase was mounted in the base of the cell, while the probe electrode, a 1-μm diameter glass-coated Pt disk UME, was positioned directly above it (Figure 5). The cell contained 1.0 M aqueous sulfuric acid as the receptor phase. The UME was biased at 1.2 V vs AgQRE to oxidize any MA which entered the aqueous phase at a diffusion-controlled rate. Two typical normalized MA concentration−distance profiles, for different drop growth rates are shown in Figure 6.

As determined previously,[20b] convective diffusion in the region adjacent to the drop surface in the receptor phase may be described by the following expression:

$$\frac{\partial c_i}{\partial t} = D_i\left(\frac{\partial^2 c_i}{\partial r^2} + \frac{2}{r}\frac{\partial c_i}{\partial r}\right) - \nu_r \frac{\partial c_i}{\partial r} \qquad (5)$$

where, c_i and D_i are the concentration and diffusion coefficient of the species of interest, i (Ce(IV) here). The radial coordinate from the drop center is denoted by r, and υ_r is the velocity given by

$$\nu_r = \frac{q}{4\pi}\left(\frac{1}{r^2} - \frac{1}{r_0^2}\right) \qquad (6)$$

where q is the volume flow rate and r_0 is the (time-dependent) drop radius.[20b] The theoretical profiles accompanying the experimental data in Figure 6 were obtained by simulation of the convective diffusion of MA adjacent to the drop surface using eqs 5 and 6, with a no-flux boundary condition far from

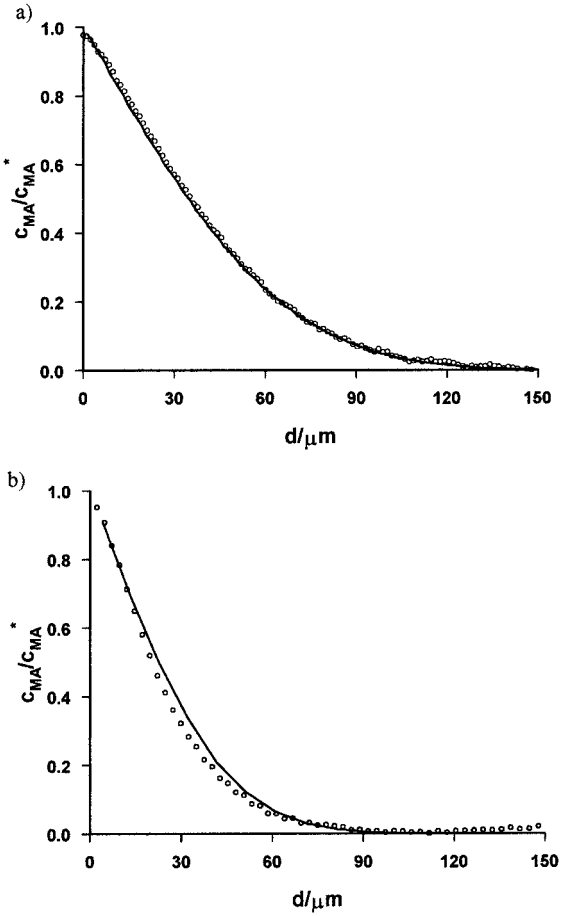

Figure 6. MA dissolution profile from a growing droplet of neat MA in 1.0 M H_2SO_4, presented as normalized concentration vs (time-dependent) distance from the drop surface (○). Drop times were (a) 7.18 s and (b) 3.59 s. The solid line indicates the simulated response for diffusion-controlled dissolution, with $D_{MA} = 4.5 \times 10^{-6}$ cm^2 s^{-1}.

the drop surface[20b] and the following boundary condition at the drop surface:

$$r = r_0: \qquad c_{MA} = c_{MA}^* \tag{7}$$

where c_{MA}^* is the saturated concentration of MA in the aqueous phase. This latter boundary condition applies to diffusion-limited MA dissolution. Data from several experiments, with drop times in the range 3−10 s yielded $c_{MA}^* = 4.3\ (\pm 0.1) \times 10^{-3}$ M, which agreed well with literature values for the solubility of MA in aqueous sulfuric acid.[4] The MA diffusion coefficient, $D_{MA} = 4.50 \times 10^{-6}$ cm s^{-1}, was used in the simulation. The observation of saturated levels of MA at the liquid/liquid interface suggests that the dissolution step is rapid on the MEMED time scale, with no interfacial transfer resistance under these conditions.

Rate of the Homogeneous Reaction of MA with Ce(IV). Having identified that the dissolution of MA is free from interfacial transfer resistances on the time scale of MEMED measurements, it was necessary to determine the rate equation for the reaction between dissolved MA and Ce(IV) in 1.0 M aqueous sulfuric acid solutions. Based on earlier studies of the oxidation of substituted methylbenzenes, the reaction is proposed to occur via the following mechanism:[8,12,13,16]

$$\mathrm{MA} + \mathrm{Ce(IV)} \underset{k_{h-1}}{\overset{k_{h1}}{\rightleftharpoons}} \mathrm{MA}^{+\bullet} + \mathrm{Ce(III)} \tag{8}$$

$$\mathrm{MA}^{+\bullet} \xrightarrow{k_{h2}} \mathrm{MA}^{\bullet} + \mathrm{H}^+ \tag{9}$$

$$\mathrm{MA}^{\bullet} + \mathrm{Ce(IV)} \xrightarrow{k_{h3}} \text{products} \tag{10}$$

where $MA^{+\bullet}$ is the cation radical, the lifetime of which we have already determined by UME voltammetry, with a rate constant, k_{h2} in eq 9, of 77 or 154 s^{-1}. $MA^{\bullet}$ is the radical product of the deprotonation reaction, which should undergo rapid oxidation, by either Ce(IV) or $MA^{+\bullet}$, based on the earlier voltammetric analysis, which demonstrated that $MA^{\bullet}$ is more readily oxidized than MA. The products formed in this process can also be further oxidized (see scheme in Figure 1), but this was not important on the time scale of the homogeneous kinetic studies or the MEMED studies which follow.

The overall kinetics of the solution reaction were followed simply by measuring the initial rate of reaction immediately following the mixing of aqueous sulfuric acid solutions of MA and Ce(IV) of known initial concentration ($[MA]_{initial}$ in the range 0.50−1.50 mM, and $[Ce(IV)]_{initial}$ in the range 0.015−0.150 mM). The reaction was probed by measuring the concentration of Ce(IV) spectrophotometrically via the absorbance at 320 nm. The molar absorptivity was determined over the range of [Ce(IV)] of interest, $\epsilon = 4.95 \times 10^6$ cm^2 mol^{-1}, enabling the Ce(IV) concentration to be calculated from the Beer−Lambert law. The following rate expression for the overall reaction was determined:[34]

$$-\frac{\mathrm{d}c_{\mathrm{Ce(IV)}}}{\mathrm{d}t} = -2\frac{\mathrm{d}c_{\mathrm{MA}}}{\mathrm{d}t} = k_{\mathrm{hom}} c_{\mathrm{Ce(IV)}} c_{\mathrm{MA}} \tag{11}$$

where the rate constant, $k_{hom} = 1.0\ (\pm 0.2) \times 10^{-3}$ mol^{-1} m^3 s^{-1}.

The rate law determined in these studies suggests that the rate-determining step for the homogeneous reaction defined in eqs 8−10 is likely to be the initial electron-transfer step (eq 8) and that subsequent steps are comparatively rapid. This observation contrasts with the results of other oxidation reactions of substituted methylbenzenes by metal ions in solution, where the second step (eq 9 in this case) was identified as the slow step.[8−12] However, the conditions of interest herein are distinctly different from those in these previous studies, which employed contrasting solvents and oxidants.

MEMED Measurements: Interfacial versus Homogeneous ET. The redox reaction between Ce(IV) and MA in a two-phase liquid system was measured by MEMED, by determining the concentration profiles of both species as a droplet of MA expanded toward a UME in an aqueous phase containing 1.0 M sulfuric acid and Ce(IV) at a concentration of 5×10^{-3} M. The Ce(IV) profile was measured by biasing the 1-μm diameter Pt UME at 0.0 V vs AgQRE during the period of one drop and recording the current for Ce(IV) reduction. The potential was then switched to 1.2 V vs AgQRE in order to record the MA dissolution profile on a subsequent drop.

Typical MA and Ce(IV) concentration profiles are shown in Figure 7, for a drop time of 6.08 s. The MA profile is little changed from the diffusion-limited dissolution case (solid line theory), while the Ce(IV) profile can be seen to decrease significantly near to the drop surface. This is not simply due to transfer of Ce(IV) to the MA phase, since control experiments carried out under similar conditions, but with an organic droplet of 1,2-dichloroethane, showed little change in the Ce(IV) concentration near the droplet, until the electrode was less than 4 μm from the surface, when diffusion of Ce(IV) to the UME

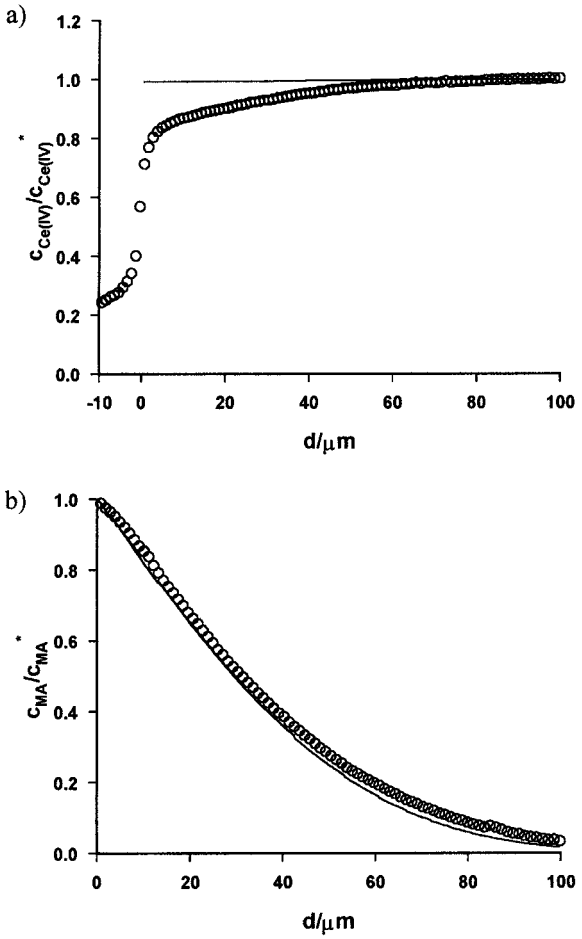

Figure 7. Concentration profiles for the two-phase reaction between an aqueous receptor phase containing Ce(IV) at a concentration of 5×10^{-3} M in 1.0 M H_2SO_4 and an MA feeder phase. The drop time was 6.08 s. (a) Ce(IV) concentration profile; (b) MA concentration profile. The solid line in (a) represents the theoretical profile for diffusion-controlled MA dissolution followed by the homogeneous reaction of MA with Ce(IV), with $k_{hom} = 1 \times 10^{-3}$ mol^{-1} m^3 s^{-1}, while that in (b) is the theoretical profile for diffusion-controlled MA dissolution.

in the aqueous phase was hindered by the presence of the drop.[20b] Given the huge hydration enthalpy, $\Delta_{hyd}H = 6688.5$ kJ/mol of Ce(IV),[35] its transfer from water to the organic phase is highly unlikely. Moreover, since the solubility of DCE in water is much higher than that of MA in water,[36] the fact that we do not see Ce(IV) transfer in the DCE/water system means that it is unlikely in the case of MA/water.

Based on the results in the preceding section, a model that described the purely homogeneous reaction of MA with Ce(IV) in the MEMED arrangement was developed, to compare with the experimental results. The model, which required consideration of both the MA and the Ce(IV) species, was formulated taking into account the following two reactions:

$$MA_{drop} \xrightarrow{rapid} MA_{aq} \tag{12}$$

$$MA_{aq} + 2Ce(IV)_{aq} \xrightarrow{k_{hom}} \text{products} \tag{13}$$

These two processes have been fully characterized above, and so the theoretical concentration profiles could be generated with no unknown parameters, using the following boundary conditions at the interface for MA and Ce(IV), respectively:

$$r = r_0: \qquad c_{MA} = c_{MA}^* \tag{14}$$

$$r = r_0: \qquad D_{Ce(IV)} \frac{\partial c_{Ce(IV)}}{\partial r} = 0 \tag{15}$$

The initial condition is that for all $r > r_0$, the concentrations of MA and Ce(IV) are $c_{MA} = 0$ and $c_{Ce(IV)} = c_{Ce(IV)}^*$, the bulk solution values.

The rate law for the homogeneous reaction is defined by eq 11, and so the convective−diffusion equations for Ce(IV) and MA in the receptor phase in the MEMED arrangement are

$$\frac{\partial c_{Ce(IV)}}{\partial t} = D_{Ce(IV)}\left(\frac{\partial^2 c_{Ce(IV)}}{\partial r^2} + \frac{2}{r}\frac{\partial c_{Ce(IV)}}{\partial r}\right) - \nu_r \frac{\partial c_{Ce(IV)}}{\partial r} - k_{hom} c_{Ce(IV)} c_{MA} \tag{16}$$

$$\frac{\partial c_{MA}}{\partial t} = D_{MA}\left(\frac{\partial^2 c_{MA}}{\partial r^2} + \frac{2}{r}\frac{\partial c_{MA}}{\partial r}\right) - \nu_r \frac{\partial c_{MA}}{r} - \frac{1}{2} k_{hom} c_{Ce(IV)} c_{MA} \tag{17}$$

Equations 16 and 17 were solved with eqs 14 and 15 as the boundary conditions, to simulate concentration profiles for both Ce(IV) and MA.

The theoretical Ce(IV) concentration profile in Figure 7a was generated by using the model described above, with the k_{hom} value deduced earlier. The model predicts a negligible change in the Ce(IV) concentration, indicating that, under these experimental conditions, a mechanism involving diffusion-limited MA dissolution, followed by homogeneous oxidation in the aqueous phase, does not adequately describe the experimentally observed depletion of Ce(IV) close to the interface ($d < 60$ μm). The MA profile showed little deviation from the pure dissolution case under these conditions of relatively slow homogeneous reaction.

Based on the above observations, the measured depletion of Ce(IV) must be due to an interfacial reaction between MA and Ce(IV).

$$MA_{drop} + Ce(IV)_{aq} \xrightarrow{k_{int}} MA^{+\bullet}{}_{aq} + Ce(III)_{aq} \tag{18}$$

where k_{int} is a rate constant for the interfacial process. The follow-up solution reactions, eqs 9 and 10, are also likely to apply; however, considering the lifetime of the radical cation ($\approx$10 ms), its diffusion length, δ_D, from the interface into the aqueous phase is limited:

$$\delta_D = \sqrt{\frac{D}{k_{ECE\ or\ DISP1}}} \tag{19}$$

For a value $D = 5 \times 10^{-6}$ cm^2 s^{-1} and the measured k_{ECE} and k_{DISP1}, $\delta_D = 2.5$ or 1.8 μm, respectively. This distance is within the region close to the interface ($d < 5a$) inaccessible to the probe, due to the onset of hindered diffusion to the detector electrode, as highlighted above and described previously in detail.[20b] To the MEMED probe, the reaction of two Ce(IV) ions with one MA molecule, based on the reaction stoichiometry, thus essentially appears interfacial.

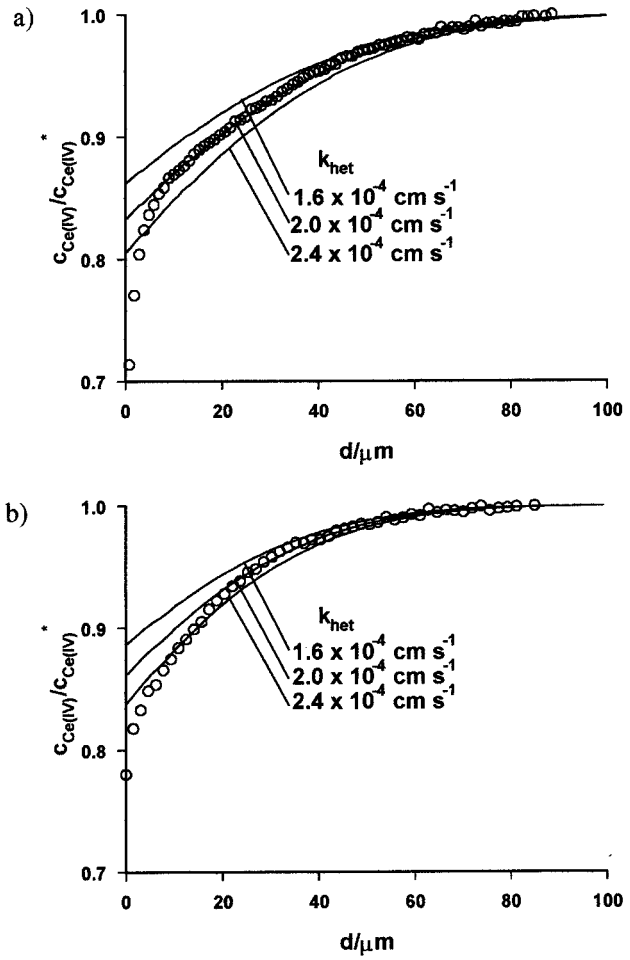

Figure 8. Ce(IV) concentration profiles recorded during reaction of Ce(IV) with MA in the MEMED arrangement, with drop times of (a) 6.08 s and (b) 3.80 s. The solid lines represent the theoretically predicted behavior based on a heterogeneous reaction at the interface with the rate constants indicated.

The reaction was modeled as such, in terms of the following boundary condition at the droplet surface:

$$-D_{Ce(IV)}\frac{\partial c_{Ce(IV)}}{\partial r} = k_{int}c_{Ce(IV)} \qquad (20)$$

Typical Ce(IV) concentration profiles for two different drop times are shown in Figure 8, along with simulations based on solving the convective−diffusion equation (eq 5), with eq 20 as the boundary condition. The experimental data are seen to match well to the model, except at the smallest *d* values where the electrode response becomes complicated by restricted diffusion of Ce(IV), due to the advancing droplet.[20b] A value for $k_{int} = 2.0\ (\pm 0.4) \times 10^{-4}$ cm s^{-1} was determined by this method. This model assumes that MA continues to dissolve at a diffusion-controlled rate, unaffected by the interfacial reaction (which proceeds at a rather slow rate), as found experimentally (see for example Figure 7b).

Discussion

Under the conditions of the MEMED studies, the predominant reaction between Ce(IV) and MA occurs interfacially, rather than by dissolution of MA followed by reaction in aqueous solution. In fact, the measurements described herein enable the interfacial reaction to be identified and probed without the influence of the solution reaction. The ability to determine both the interfacial and the homogeneous reaction rates separately makes it possible to identify how these two reaction routes would compete under a range of experimental conditions.

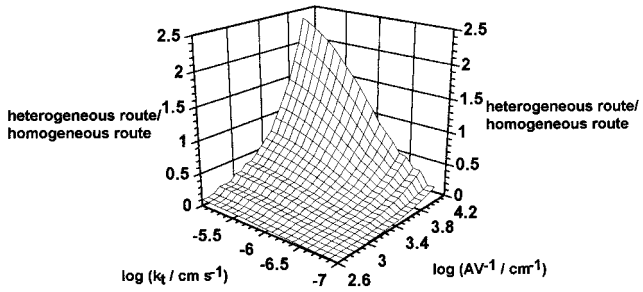

Figure 9. Kinetic indicator plot for the two-phase reaction between Ce(IV) and MA, indicating the relative importance of the heterogeneous and homogeneous reaction routes, based on eqs 21−23, as a function of the transport rate constant, k_t, and the area-to-volume ratio, AV^{-1}.

Consider the example of a reactor consisting of a suspension of stirred droplets. Figure 9 is a kinetic indicator plot for the two-phase reaction, which indicates the relative importance of the interfacial and homogeneous reaction routes in terms of key experimental parameters. The coefficient, k_t, represents transport of Ce(IV) to the interface, and AV^{-1} is the ratio of the interfacial boundary area to the volume of the aqueous solution. The upright axis represents the relative contributions of the homogeneous and interfacial routes to the overall reaction, calculated from

$$\frac{\text{interfacial route}}{\text{homogeneous route}} = \frac{\text{interfacial rate} \times AV^{-1}}{\text{homogeneous rate}} \qquad (21)$$

where the interfacial and homogeneous rates are given by

$$\text{interfacial rate} = \frac{k_{int}k_t c_{Ce(IV)}^*}{k_{int} + k_t} \qquad (22)$$

$$\text{homogeneous rate} = k_{hom}c_{Ce(IV)}^* c_{MA}^* \qquad (23)$$

In writing eq 23, it is assumed that the concentration of MA is maintained at the bulk value by the dissolution of MA. In constructing Figure 9, $c_{Ce(IV)}^* = c_{MA}^* = 5 \times 10^{-3}$ M was used as the bulk concentration for the two species. Figure 9 demonstrates that there are a wide range of conditions where the interfacial reaction route would contribute significantly to the overall process, although this route has not previously been recognized. At a general level, the ability to identify new reaction routes by MEMED, to which other techniques would be blind, may have important implications for the study of two-phase liquid reactions where competing processes are involved.

Several possible reasons could explain the difference between the expected and observed behavior. In particular, the environment at the interface is quite different to that in bulk solution. Indeed, the effect and presence of a mixed solvent region in the vicinity of the interface has been the subject of much consideration in the interpretation of electrochemical measurements[18] and has been examined experimentally[37] and through molecular dynamics simulations.[38] Based on Marcus theory for ET at a liquid/liquid interface,[39] only a small difference in the free energy of activation between the homogeneous and heterogeneous processes, $\Delta G^{\ddagger}_{hom} - \Delta G^{\ddagger}_{het}$, is required to explain the difference in the measured rate constants. The ratio

of the homogeneous and heterogeneous rate constants constants is given by

$$\frac{k_{\mathrm{hom}}}{k_{\mathrm{het}}/c_{\mathrm{MA}}^{\mathrm{droplet}}} = \frac{1}{L}\exp\left(\frac{\Delta G^{\ddagger}_{\mathrm{het}} - \Delta G^{\ddagger}_{\mathrm{hom}}}{RT}\right) \qquad (24)$$

where L is the thickness of the interfacial region and $c_{\mathrm{MA}}^{\mathrm{droplet}}$ is the MA concentration in the MA droplet, which is 8 M. R and T have their usual meaning. If $L = 1$ nm, then $(\Delta G^{\ddagger}_{\mathrm{hom}} - \Delta G^{\ddagger}_{\mathrm{het}}) = 13.7$ kJ/mol is calculated. This could be attributed to differences in either the reorganization energy and/or the redox potential of MA in the neat phase compared to that of MA in the aqueous solution, although further work will be needed to confirm this.

Conclusions

The application of MEMED to the study of the oxidation of MA by aqueous solutions of Ce(IV) in a two-phase arrangement has revealed a new interfacial route for this reaction, while the known homogeneous reaction between dissolved MA and Ce(IV) in aqueous sulfuric acid is relatively slow. It has been possible to measure rates for both the homogeneous and interfacial reaction, allowing an understanding of how these two possible reaction routes would compete under a range of experimental conditions. Moreover, the different apparent rate constants, and hence energetics for interfacial and homogeneous ET have been rationalized by using a simple treatment arising from Marcus theory.

The ability to identify new reaction routes by MEMED, to which other techniques may be blind, has important implications for the study of reaction kinetics in two-phase liquid systems, particularly where competing processes are involved and where the distribution of products may be effected by the competition between interfacial and homogeneous routes. Having demonstrated the sensitivity of the MEMED technique, in measuring reaction rates via direct visualization of interfacial concentration profiles, we envisage considerable further use of the methodology with expansion of the range of possible applications beyond those already described.[20]

Acknowledgment. We thank EPSRC and Avecia for support of this work. Helpful discussions with Dr. John Atherton are much appreciated.

References and Notes

(1) Atherton, J. H. *Res. Chem. Kinet.* **1994**, *2*, 193.
(2) Freiser, H. *Chem. Rev.* **1980**, *88*, 611.
(3) Danesi, P. R.; Chiarizia, R. *CRC Crit. Rev. Anal. Chem.* **1980**, *10*, 1.
(4) Tzedakis, T.; Savall, A. *Chem. Eng. Sci.* **1991**, *46*, 2269.
(5) Tzedakis, T.; Savall, A. J. *Ind. Eng. Chem. Res.* **1992**, *31*, 2475.
(6) Tzedakis, T.; Savall, A. J. *J. Appl. Electrochem.* **1997**, *27*, 589.
(7) Eberson, L. *J. Am. Chem. Soc.* **1983**, *105*, 3192.
(8) Baciocchi, E.; Bietti, M.; Mattioli, M. *J. Org. Chem.* **1993**, *58*, 7106.
(9) Ito, O.; Akiho, S.; Iino, M. *J. Org. Chem.* **1989**, *54*, 2436.
(10) Schlesener, C. J.; Kochi, J. K. *J. Org. Chem.* **1984**, *49*, 3142.
(11) Reed, R. A.; Murray, R. W. *J. Electroanal. Chem.* **1990**, *285*, 149.
(12) Baciocchi, E.; Rol, C.; Mandolini, L. *J. Am. Chem. Soc.* **1980**, *102*, 7597.
(13) Kreh, R. P.; Spotnitz, R. M.; Lundquist, J. T. *Tetrahedron Lett.* **1987**, *28*, 1068.
(14) Ho, T.-L. *Synthesis* **1973**, 347.
(15) Trahanovsky, W. S.; Young, L. B. *J. Org. Chem.* **1966**, *31*, 3.
(16) Torii, S.; Tanaka, H.; Inokuchi, T.; Nakane, S.; Akada, M.; Saito, N.; Sirakawa, T. *J. Org. Chem.* **1982**, *47*, 1647.
(17) Pletcher, D.; Valdes, E. M. *J. Chem. Res. (S)* **1987**, 386.
(18) (a) Girault, H. H.; Schiffrin, D. J. In *Electroanalytical Chemistry;* Bard, A. J., Ed.; Marcel Dekker: New York, 1989; Vol. 15, p 1. (b)Vanýsek, P. *Electrochim. Acta* **1995**, *40*, 2841. (c) Volkov, A. G.; Deamer, D. W., Eds. *Liquid−Liquid Interfaces: Theory and Methods*; CRC Press: Boca Raton, FL, 1996.
(19) For recent examples of ET reactions at liquid/liquid interfaces, see, for example: (a) Tsionsky, M.; Bard, A. J.; Mirkin, M. V. *J. Phys. Chem. B* **1996**, *100*, 17 881. (b) Tsionsky, M.; Bard, A. J.; Mirkin, M. V. *J. Am. Chem. Soc.* **1997**, *119*, 10 785. (c) Fermin, D. J.; Ding, Z.; Duong, D. H.; Brevet, P. F.; Girault, H. H. *J. Phys. Chem. B* **1998**, *102*, 10 334. (d) Fermin, D. J.; Duong, H. D.; Ding, Z.; Brevet, P. F.; Girault, H. H. *J. Am. Chem. Soc.* **1999**, *121*, 10 203. (e) Barker, A. L.; Unwin, P. R.; Amemiya, S.; Zhou, J.; Bard, A. J. *J. Phys. Chem. B* **1999**, *103*, 7260. (f) Cunnane, V. J.; Geblewicz, G.; Schiffrin, D. J. *Electrochim. Acta* **1995**, *40*, 3005. (g) Cheng, Y. F.; Schiffrin, D. J. *J. Chem. Soc., Faraday Trans.* **1993**, *89*, 199.
(20) (a) Slevin, C. J.; Unwin, P. R. *Langmuir* **1997**, *13*, 4799. (b) Slevin, C. J.; Unwin, P. R. *Langmuir* **1999**, *15*, 7361. (c) Zhang, J.; Slevin, C. J.; Unwin, P. R. *Chem. Commun.* **1999**, 1501. (d) Zhang, J.; Unwin, P. R. *J. Phys. Chem. B* **2000**, *104*, 2341. (e) Zhang, J.; Unwin, P. R. *Phys. Chem. Chem. Phys.* **2000**, *2*, 1267. (f) Zhang, J.; Barker, A. L.; Unwin, P. R. *J. Electroanal. Chem.* **2000**, *483*, 95. (g) Zhang, J.; Slevin, C. J.; Murtomäki, L.; Kontturi, K.; Williams, D. E.; Unwin, P. R. *Langmuir* **2001**, *17*, 821.
(21) Slevin, C. J.; Unwin, P. R.; Zhang, J. In *Liquid/interfaces in Chemical, Biological and Pharmaceutical Applications*; Volkov, A. G., Ed.; Marcel Dekker: New York, 2000; pp 325−354.
(22) Hanna, G. J.; Noble, R. D. *Chem. Rev.* **1985**, *85*, 583.
(23) Marcus, R. A. *J. Phys. Chem.* **1990**, *94*, 1050.
(24) Schmickler, W. *J. Electroanal. Chem.* **1997**, *428*, 123.
(25) Wightman, R. M.; Wipf, D. O. In *Electroanalytical Chemistry*; Bard, A. J., Ed.; Marcel Dekker: New York, 1989; Vol. 15, p 267.
(26) Saito, Y. *Rev. Polarogr. Jpn.* **1968**, *15*, 177.
(27) Randle, T. H.; Kuhn, A. T. *J. Chem. Soc., Faraday Trans. 1* **1983**, *79*, 1741.
(28) Bard, A. J.; Faulkner, L. R. *Electrochemical Methods, Fundamentals and Applications*; John Wiley and Sons: New York, 1980.
(29) (a) Hawley, M. D.; Feldberg, S. W. *J. Phys. Chem.* **1966**, *70*, 3459. (b) Andrieux, C. P.; Savéant, J.-M. *J. Electroanal. Chem.* **1989**, *267*, 15. (c) Amatore, C.; Gareil, M.; Savéant, J.-M. *J. Electroanal. Chem.* **1983**, *147*, 1.
(30) Hlavatý, J. *J. Appl. Electrochem.* **1994**, *24*, 989.
(31) Parker, V. D.; Adams, R. N. *Tetrahedron Lett.* **1969**, *21*, 1721.
(32) Marquez, J.; de Marquez, O. P. *Rev. Roum. Chem.* **1993**, *38*, 775.
(33) Fleischmann, M.; Lasserre, F.; Robinson, J. *J. Electroanal. Chem.* **1984**, *177*, 115.
(34) Slevin, C. J. Ph.D. Thesis, University of Warwick, 1999.
(35) Richens, D. T. *The Chemistry of Aqua Ions*; Wiley: Chichester, 1997.
(36) The Merck Index, Merck, Whitehouse Station, NJ, 1996.
(37) Strutwolf, J.; Barker, A. L.; Gonsalves, M.; Caruana, D. J.; Unwin, P. R.; Williams, D. J.; Webster, J. R. P. *J. Electroanal. Chem.* **2000**, *883*, 163.
(38) Benjamin, I. *Chem. Rev.* **1996**, *96*, 1449.
(39) Marcus, R. A. *J. Phys. Chem.* **1991**, *95*, 2010.